High Hcy regulates fluid shear stress pathway activity through histone H3K79 homocysteinylation in hyperhomocysteinemia-related child hypertension

Baoling Bai[1†], Lingyun Liu[1†], Yanyan Liu[2†], Shuangshuang Yang[1], Haojie Wu[2], Kexin Zhang[1], Lin Shi[2*] and Qin Zhang[1*]

Abstract

Background The rise of hypertension in children has been increasingly associated with hyperhomocysteinemia (HHcy), which is recognized as a major risk factor. However, the underlying mechanisms linking homocysteine and hypertension (termed HHYP) are not fully understood.

Methods This study utilized plasma samples from 27 control children and 27 children with HHYP (aged 8 ~ 16 years) for TMT6-labeled proteomic quantification, identifying significant altered proteins. Bioinformatics analysis revealed pathway alterations. Verification was carried out via parallel reaction monitoring (PRM) and western blot (WB) analyses. Additionally, a rat model of HHYP induced by high methionine diets, and umbilical vein endothelial cell models exposed to high homocysteine (hcy) levels were developed to investigate the molecular underpinnings further. Protein expression changes and epigenetic modifications were assessed using WB, immunohistochemistry (IHC), and ChIP-qPCR techniques.

Results Key findings indicated that 357 proteins and 69 pathways were altered in children with HHYP. Specifically, 12 proteins within the fluid shear stress and atherosclerosis (FSSA) pathway showed differential expression, including the downregulation of TRX1 and GPX1 and the upregulation of ICAM1. The same expression patterns were noted in both the HHYP rat aortic tissues and the high hcy cultured endothelial cells. Moreover, elevated H3K79hcy modification levels were observed alongside epigenetic regulation of genes related to the FSSA pathway. Importantly, folic acid

---

†Baoling Bai, Lingyun Liu and Yanyan Liu contributed equally to this work.

*Correspondence:
Lin Shi
shilin9789@126.com
Qin Zhang
zhangqin87@pumc.edu.cn

Full list of author information is available at the end of the article

Bai *et al. Journal of Translational Medicine*   (2025) 23:525

Page 2 of 17

(FA), a medication frequently used in the clinical treatment of HHYP, has been demonstrated to effectively reverse H3K79hcy modifications and restore the disrupted FSSA pathway in both animal models and cell cultures.

Conclusions The present study suggests that HHcy may contribute to hypertension through the epigenetic dysregulation of the FSSA pathway mediated by H3K79hcy. Furthermore, the pediatric proteomics data gleaned from this study offer new clinical insights into the pathophysiology of HHYP in children.

Keywords Hyperhomocysteinemia (HHcy), HHcy-type hypertension (HHYP), TMT-6plex labeling, Fluid shear stress and atherosclerosis (FSSA), H3K79hcy

Background

Pediatric hypertension is characterized by systolic blood pressure (SBP) or diastolic blood pressure (DBP) levels at or above the 95th percentile for a healthy child population [1]. Evolving lifestyle factors have contributed to an increasing prevalence of hypertension among children. In Asian countries, pediatric hypertension has become more widespread than ever before [2]. A study conducted in China examined 128,113 students aged 6 ~ 17 years, finding that 13.56% exhibited hypertension, with a higher incidence in boys compared to girls [3]. Hypertension serves as a prominent risk factor for cardiovascular diseases and chronic kidney diseases globally [4]. It predisposes individuals to the development of left ventricular hypertrophy, heart failure, stroke, aneurysm, and other vascular and cardiac pathophysiologies [5]. Consequently, early prevention and intervention are crucial for ensuring the healthy development of children.

Hypertension is a multifactorial condition, and its association with hyperhomocysteinemia (HHcy) has been well-established [6, 7]. The concomitant presence of HHcy and hypertension, known as HHYP, is characterized by elevated serum homocysteine (Hcy) levels of 15.0 μM or higher and has been identified in 60% of hypertensive individuals based on blood test results [8].

Factors contributing to HHcy include diminished activities of enzymes such as methyltetrahydrofolate reductase (MTHFR) and cystathionine β-synthase, deficiencies in folate or cofactors like vitamins B6/B12. Among these, folate deficiency can lead to an excess of methionine and subsequently result in HHcy [9, 10], which is considered the most prevalent cause of HHcy [11]. Personalized administration of folic acid (FA) tablets has been shown to effectively reduce blood pressure, homocysteine levels, and coagulation factors, while also significantly improving pro-thrombotic status in patients with HHYP [12, 13].

The pathological mechanism underlying HHYP is complex. Compelling evidence suggests that HHcy can trigger vascular inflammation by upregulating the expression levels of interleukin-6 (IL-6) and nuclear factor-kappa B (NFκB) p65/RelA [10]. Furthermore, HHcy has been shown to limit nitric oxide (NO) bioavailability and promote oxidative injury to the endothelium. Utilization of antioxidants to reduce oxidative stress has been proposed as a potential adjuvant therapy for essential hypertension [13], indicating that HHcy may also contribute to hypertension through the elevation of oxidative stress. Additionally, Hcy can be synthesized into homocysteine thiolactone (HTL) under the catalysis of the methionine

Table 1 Clinical characteristics of children for TMT6-labled quantification

Groups	Con	HHYP	*P* value
Cases, n	27	27	—
Male, n	27	27	>0.999
Age (± s, years)	12.61 ± 0.46	13.46 ± 0.11	0.081
sSBP (± s, mmHg)	108.26 ± 8.64	139.98 ± 9.64	<0.001
sDBP (± s, mmHg)	62.54 ± 4.95	79.97 ± 8.21	<0.001
BMI (± s, kg/m2)	21.11 ± 1.14	28.08 ± 1.05	<0.001
Cholesterol (mmol/L)	4.01 ± 0.18	4.45 ± 0.15	0.071
TG (mmol/L)	1.17 ± 0.11	1.59 ± 0.21	0.091
HDL (mmol/L)	1.28 ± 0.06	1.10 ± 0.06	0.035
LDL (mmol/L)	2.38 ± 0.18	3.05 ± 0.16	0.007

sSBP: mean supine systolic blood pressure

sDBP: mean supine diastolic blood pressure

BMI: body mass index

TG: triglyceride

HDL: High density lipoprotein
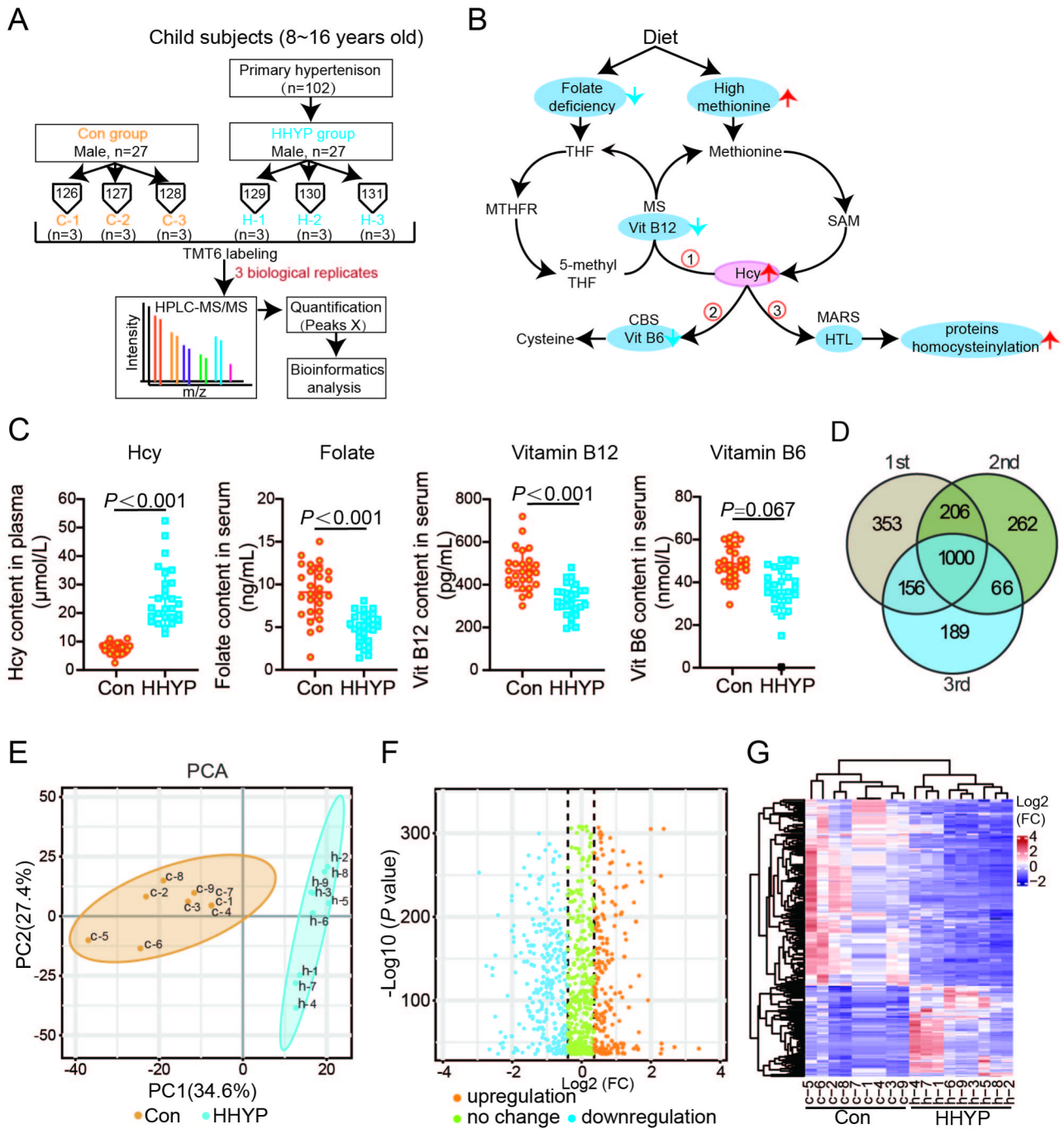
LDL: Low-density lipoprotein

Fig. 1 TMT-6plex quantification results. (**A**) A schematic diagram of the sample grouping information and the TMT6 labeling quantitative process. (**B**) Homocysteine metabolic chart, where a diet low in folate or high in methionine can lead to elevated levels of Hcy, which can further be metabolized into homocysteine thiolactone (HTL) under the catalysis of MARS enzymes. The latter can cause homocysteinylation modifications of histones or proteins. (**C**) The plasma contents of Hcy, serum contents of folate, and vitamin B12/6. (**D**) The Venn diagram displays the number of proteins detected in three biological replicates of TMT6 labeling quantification. (**E**) Principal component analysis (PCA) analysis of the control and HHYP TMT6 quantification data globally. (**F**) Volcano plot shows the 1000 proteins in the plasma of patients, proteins with fold change > 1.3 difference in HHYP compared to controls is shown in blue (upregulated) and orange plots (upregulated). The horizontal dashed grey line represents the selected significance threshold. The vertical broken grey lines correspond to the upregulated and downregulated fold change thresholds. (**G**) Heatmap displays the protein expression intensity averaged across individuals

tRNAsynthetase (MARS) enzyme, the latter of which can lead to protein homocysteinylation, subsequently altering the expression of blood clotting-related genes, thereby disrupting vascular homeostasis and affecting the

endothelium [14, 15]. Further investigation is required to elucidate the precise mechanisms of Hcy-induced vascular endothelial damage and its contribution to atherosclerosis and other vascular diseases.

In a previous study, we investigated the potential mechanisms of HHYP from a metabolomics perspective [16]. In this project, we aim to further enhance our understanding of the pathological mechanisms underlying HHYP by examining it from a proteomics standpoint. We collected plasma samples from 27 pediatric patients with HHYP. Utilizing the tandem mass tag (TMT) 6-plex labeling quantification method, we obtained differentially expressed protein profiles to identify proteins that may influence HHYP and further investigate their potential biological functions. Additionally, we validated these altered proteins using a hypertensive rat model with hyperhomocysteinemia induced by methionine feeding. Combined with a high Hcy-treated umbilical vein endothelial cell model, we explored the molecular mechanisms of high Hcy-induced hypertension.

Materials and methods
Human subjects
We have screened 27 cases of hyperhomocysteinemia-type hypertension from a total of 102 primary hypertension samples which were collected in our hospital in 2021, presented at the cardiology outpatient clinic. Inclusion criteria: Primary hypertension with plasma Hcy content>10μM. We also recruited 27 controls who came to the clinic for a health examination. Controls had no history of diabetes mellitus, secondary hypertension, myocardial infarction, stroke, renal failure, drug abuse or other serious diseases, and no family history of hypertension in first-degree relatives.

Animals
36 male Sprague–Dawley (SD) rats were obtained from the Beijing Vital River Laboratory Animal Center (Beijing, China). They were randomly divided into three experimental groups: Control group, HHYP group and HHYP + FA group ($n = 12$/group). The control group was fed with rat maintenance formula feed (contains 5.80 g methionine, 6.60 mg FA per 1 kg) for 16 weeks; HHYP group rats were fed with 7.7 g/kg methionine diet for 16 weeks; Rats at 12th week in HHYP group subsequently fed with 7.7 g/kg methionine + 100 mg/kg FA (F7876, Sigma) for 4 weeks were divided into HHYP + FA group.

Blood pressure measurement of rats
SBP and DBP of rat tail artery were monitored at the same time of day with a noninvasive BP measurement system (Beijing Ruolong Biotechnology, BP-2000) under rat conscious state. Hypertension is classified as G1 and G2. All rats were tested for BP at least every 1 week after the 5th week study.

Measurement of Hcy and B vitamins
All children or rats were fasted 12 h beforehand, and plasma samples were collected and sent to the laboratory of our hospital for testing hcy, serum folate and vitamin B12/6 concentrations by cobase 601 automatic biochemical analyzer (Roche, Switzerland) according to the manufacturer's instructions.

In-solution tryptic digestion, TMT-6plex labeling and protein identification and quantification analysis
Firstly remove the high abundance protein of plasma according to the High-select Top14 abundant protein depletion resin (Thermo Scientific™, A36370) manufacturer's instructions. 50 μg plasma protein were reduced by TCEP at 55℃ for 1 h, alkylated by iodoacetamide for 30 min, then add 1.25μL trypsin per 50 μg of protein for digestion overnight at 37℃. Obtained peptides were labeling with TMT-6plex kit (Thermo Scientific, 90066). Then, the six labeled samples were mixed equally in a new micro-centrifuge and the samples were cleaned with a C18 spin probe (Thermo Scientific, 87784). Finally, fractionation of the peptide mixture by high pH one-dimensional reverse phase chromatography was performed on a Dionex Ultimate 3000 HPLC system, as described in our previously study [17], trypsin digest at 200 μl/ min flow rate was injected into the phenomenex column (Gemini NX 3U C18 110 A; 1502.00 mm). Fractions were collected every 1.5 min during the course of the run. Subsequently, all 40 collected fractions were mixed into 10 components, lyophilized, and kept at – 80 ∘C for further Nano- HPLC/MS/MS analysis.

Raw data were searched against the Homo sapiens database (www.uniprot.org, UP00005610) using Peaks X Studio (Version 10.0, BSI). The precursor ion mass error tolerance was set to 10 ppm, and the fragment ion mass error tolerance was 0.02 Da. Peptide spectral matches were verified at a 1% false discovery rate (FDR) using a q-value-based filter. Post-translational modifications and chemical labeling settings included fixed cysteine alkylation and TMT-6plex. Protein unique peptides were set to greater than 1, and high confidence scores (– 10logP > 20) were considered as accurately identified. The differential proteins between the HHYP and CON groups were evaluated by Student's two-tailed t-test.

Parallel reaction monitoring (PRM), Western blotting (WB) and immunohistochemistry (IHC) verifications
For PRM, the MS data were processed using Skyline (version 3.5.0.9319; AB Sciex). For each peptide, transition peak areas were normalized by the average of the sum of the transition peak areas for all the peptides across the

runs [17]. For WB, protein samples (10 µg per lane) were separated by 4–12% NuPAGE™ Bis-Tris (Thermo Scientific™, NP032B) and further incubated with primary antibodies (Anti-TRX1, CST, 2429; Anti-ICAM1, Abcam, ab282575; Anti-GPX1, CST, 3206; Anti-Albumin, CST, 4929; Anti-Gapdh, CST, 5174) overnight at 4 ℃. In addition, aortic tissues of rats were pre-fixation with 4% paraformaldehyde after dissection for IHC analysis.

Human umbilical vein endothelial cell culture and drug treatment
The EA.hy926 cell cells were purchased from the cell bank of Peking Union Medical College Hospital, with a culture medium composed of 90% DMEM (10566016, Gibco) and 10% serum. Cells are cultured in a 37 ℃ humidified environment with 5% CO_2, and the passage ratio is 1:2 to 1:3. After starvation treatment (using 1% FBS medium for 24 h), cells treated with high methionine, high Hcy, and high HTL had respective concentrations of 500 micromoles per liter; folate treatment concentration was 10 mg/L, then followed by cultivation in complete medium with the drugs for another 24 h before collection for subsequent experimental validation.

Plasmid construction and cell transfection
MARS-siRNA (Sangon, Shanghai, China) were transfected using Lipofectamine 3000 (L3000075, Thermofisher) according to the manufacturer's instructions. The transfection efficiency was measured using Immunofluorescence or western blotting.

Immunofluorescence (IF)
First, cells were rinsed three times using 1× PBS and then subjected to the following treatment steps: Cells were fixed with 0.5% paraformaldehyde for a duration of 15 min, followed by permeabilization using 0.1% Triton X-100 for 20 min at room temperature. Blocking was performed in 1× PBS containing 5% 5% bovine serum albumin (BSA), which lasted for 60 min. Overnight incubation at 4 ℃ took place with the cells being exposed to a MARS or H3K79hcy antibody that was diluted in 5% BSA. Subsequent to washing, Alexa Fluor 488-conjugated secondary antibodies (ab150077, Abcam) were applied for a 1-hour period at room temperature away from light. The nuclei received counterstaining with DAPI, and the images were obtained using a Zeiss LSM710 confocal microscope.

ChIP-qPCR and RT-qPCR
SimpleChIP® Enzymatic Chromatin IP Kit (CST, USA) was used for the H3K79hcy-ChIP assays. Total RNA was extracted from the homogenate of fresh-frozen aorta tissue using TRIzol reagents (Invitrogen, 15596026) for genes expression analysis by RT-qPCR, primer sequence

is shown in Supplementary Table 6. Result were calculated according to the cycle threshold ($2^{-\triangle\triangle Ct}$) method.

Statistical analysis
Data are expressed as means ± SEM. Difference between controls and HHYP was evaluated by Student's two-tailed *t*-test; difference among rat groups were examined by one-way ANOVA test. All statistical analyses were performed using SPSS software version 25.0.Values of $P < 0.05$ were considered statistically significant.

Results
Identification of differentially expressed plasma proteins using TMT-6plex labeling and HPLC-MS/MS
We initially collated and summarized the clinical information of 27 samples from each group, as presented in Table 1; Fig. 1A. The CON (control) group was matched with the HHYP group for age and gender. However, compared to the CON group, the HHYP group exhibited a significantly higher Body Mass Index (BMI), as well as markedly elevated SBP and DBP levels. Additionally, lipid profile analysis revealed that the HDL (High-Density Lipoprotein) cholesterol level in the HHYP group was significantly reduced, while the LDL (Low-Density Lipoprotein) cholesterol level was significantly increased, suggesting an elevated risk of cardiovascular diseases among patients in the HHYP group. Furthermore, in line with our objective to investigate the pathogenesis of hypertension associated with Hcy, we also measured levels of nutrients related to Hcy metabolism. For the HHYP cases, the plasma Hcy content was 25.35 ± 2.34µM, while for the control subjects, it was 7.61 ± 0.72µM ($P < 0.001$). Notably, serum folate and vitamin B12 levels were significantly lower in the HHYP group compared to the control group, while no change was observed in B6 levels (Fig. 1B-C), this suggests that in pediatric HHYP, the relative deficiency of folate and B12 may be the primary nutritional factors leading to elevated Hcy levels.

Subsequently, we randomly divided the 27 samples into three groups, each consisting of nine samples. These samples were then further randomly assigned into three subgroups, with each subgroup undergoing TMT labeling, followed by three biological replicates (Fig. 1A). A total of 2,232 proteins annotated in the UniProt database were identified across all samples, with 1,000 proteins common to all samples as shown in the Venn diagram of Fig. 1D. Comprehensive quantitative protein data can be found in Supplementary Table 1. Principal component analysis (PCA) was employed to evaluate the dataset, with samples evenly distributed into two distinct groups (Fig. 1E). Additionally, the volcano plot for the 1,000 proteins commonly expressed across all samples is presented in Fig. 1F. Proteins must be detected in all three biological replicates, with a fold change (HHYP/CON) greater
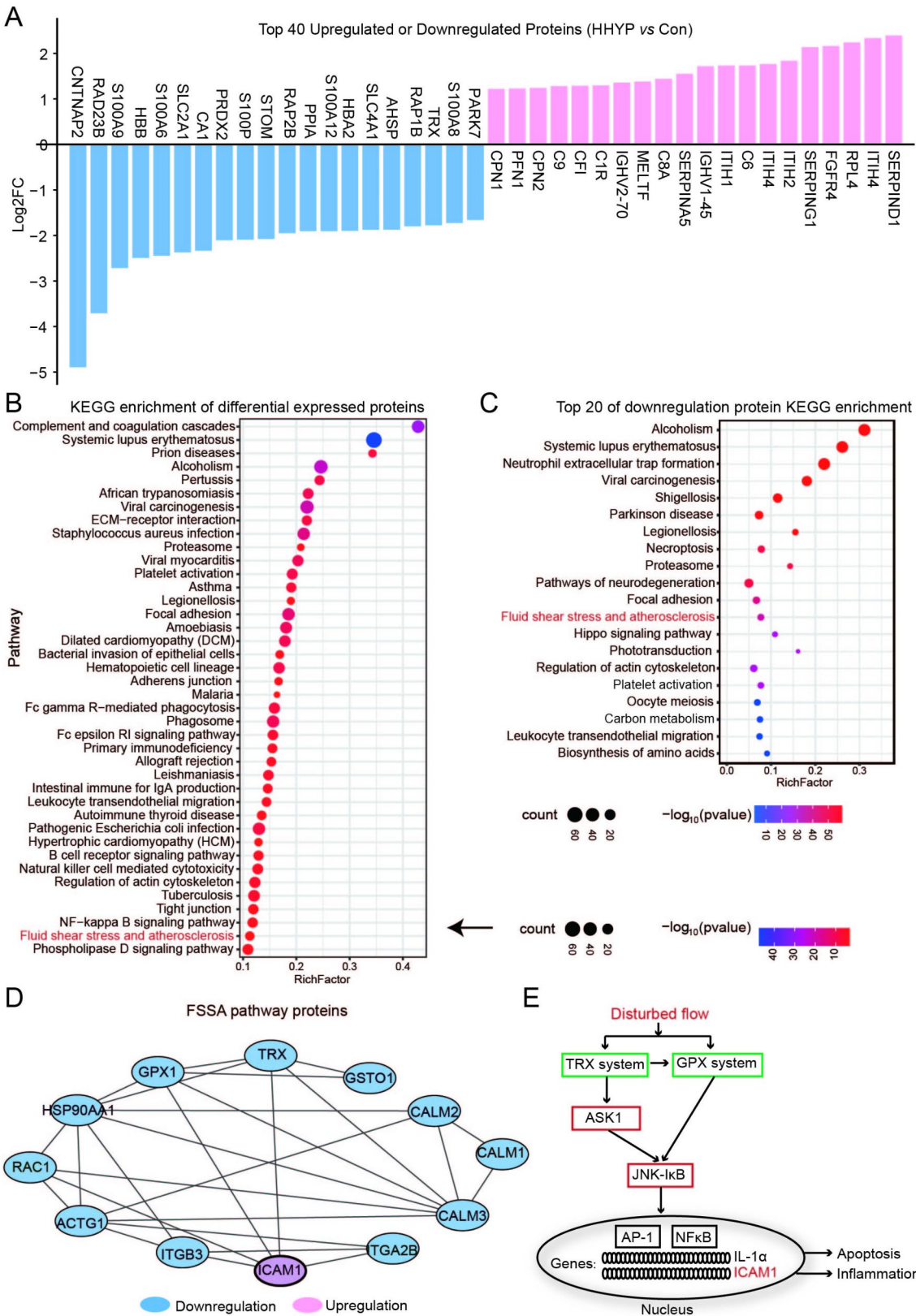
Fig. 2 (See legend on next page.)

(See figure on previous page.)

Fig. 2 Bioinformatics analysis of the 357 differentially expressed proteins in male HHYP children. (**A**) Top 40 proteins with upregulated or downregulated expression in HHYP. Top 40 pathways of all altered (**B**) and downregulated (**C**) differential proteins' KEGG classifications were displayed, respectively. The red dots denote HHYP-related pathways with P value < 0.05. (**D**) The networks analysis of the differentially expressed proteins related to FSSA pathway was carried out using String software and Cytoscape. The confidence value is set at 0.9 and the node degree ≥ 1. (**E**) Schematic diagram of the pathway under disturbed fluid shear stress, where green boxes represent inhibition and red boxes indicate activation

than 1.3 and a *p*-value less than 0.05 were considered differentially expressed. In summary, 357 proteins displayed differential expression in HHYP patients, including 103 up-regulated and 254 down-regulated proteins (Supplementary Table 2). These differentially expressed proteins then underwent unsupervised clustering, revealing a tendency for them to be preferentially assigned to corresponding groups, as indicated in Fig. 1G. This suggests common differences among HHYP patients. These findings indicate that extensive proteome alterations occur during the onset and progression of HHYP.

Bioinformatics analysis suggests the presence of FSSA pathway disruption in pediatric HHYP

To explore the potential functions of the 357 altered proteins in HHYP, we first displayed the top 20 proteins with significantly decreased or increased expression in the HHYP group in Fig. 2A. Among those with decreased expression are members of the S100 protein family that are closely related to calcium binding and regulation of intracellular signal transduction; proteins from the GTPase family such as RAP1/2B; and proteins associated with antioxidant processes like PRDX2 and TRX. Proteins with increased expression include several involved in immune and inflammatory responses, such as C1R, C6, ITIH, etc. These findings underscore the multifaceted nature of HHYP pathophysiology, suggesting

potential targets for further research and therapeutic intervention. Subsequently, we classified and annotated all differentially expressed proteins using Gene Ontology (GO) analysis. These proteins are mainly associated with cellular components and may play roles in binding and catalysis within intracellular processes and biological regulation (Supplementary Fig. 1A). Furthermore, leveraging the Kyoto Encyclopedia of Genes and Genomes (KEGG) database, we performed a comprehensive pathway enrichment analysis of these differentially expressed proteins; among 243 related pathways, 69 showed significant alterations under HHYP conditions ($P < 0.05$) (Supplementary Table 3; Fig. 2B), indicating a broad range of protein pathway modifications in patients with HHYP. Upon detailed investigation of the pathways enriched by upregulated and downregulated proteins, it was found that upregulated proteins predominantly aggregated in pathways pertaining to the immune system and NFκB signaling (Supplementary Fig. 1B). In contrast, pathways enriched by downregulated proteins include focal adhesion, hippo signaling pathway, platelet activation, and so on. We also noted that a subset of 11 proteins, including TRX, GSTO1 and HSP90AA1 among others, were markedly suppressed in the pathway related to fluid shear stress and atherosclerosis (FSSA). However, another protein in this pathway, intercellular adhesion molecule-1 (ICAM1), exhibited a notably increased expression

Table 2 Clinical characteristics of children for Western blotting validation

Groups	Con	HP	HHYP	*P* value
Cases, n	8	8	8	—
Male, n	8	8	8	>0.999*; >0.999#; >0.999&
Age (± s, years)	10.12 ± 0.96	10.75 ± 1.71	13.37 ± 0.65	0.699*; 0.055#; 0.115&
sSBP (± s, mmHg)	102.50 ± 3.20	129.75 ± 3.49	139.50 ± 5.18	<0.001*; <0.001#; 0.104&
sDBP (± s, mmHg)	66.00 ± 2.91	76.00 ± 4.33	80.00 ± 4.78	0.098*; 0.024#; 0.496&
BMI (± s, kg/m2)	17.33 ± 0.67	21.16 ± 0.89	21.78 ± 0.54	0.001*; <0.001#; 0.552&
Cholesterol (mmol/L)	3.70 ± 0.19	3.54 ± 0.18	4.18 ± 0.22	0.571*; 0.109#; 0.065&
TG (mmol/L)	0.85 ± 0.10	1.19 ± 0.24	1.32 ± 0.21	0.235*; 0.105#; 0.642&
HDL (mmol/L)	1.49 ± 0.12	1.11 ± 0.68	1.06 ± 0.77	0.008*; 0.003#; 0.707&
LDL (mmol/L)	2.07 ± 0.17	2.12 ± 0.17	2.82 ± 0.23	0.845*; 0.011#; 0.017&
Hcy (μM)	4.94 ± 1.25	7.25 ± 0.36	23.58 ± 4.32	0.537*; <0.001#; <0.001&

sSBP: mean supine systolic blood pressure

sDBP: mean supine diastolic blood pressure

BMI: body mass index

TG: triglyceride

HDL: High density lipoprotein

LDL: Low-density lipoprotein

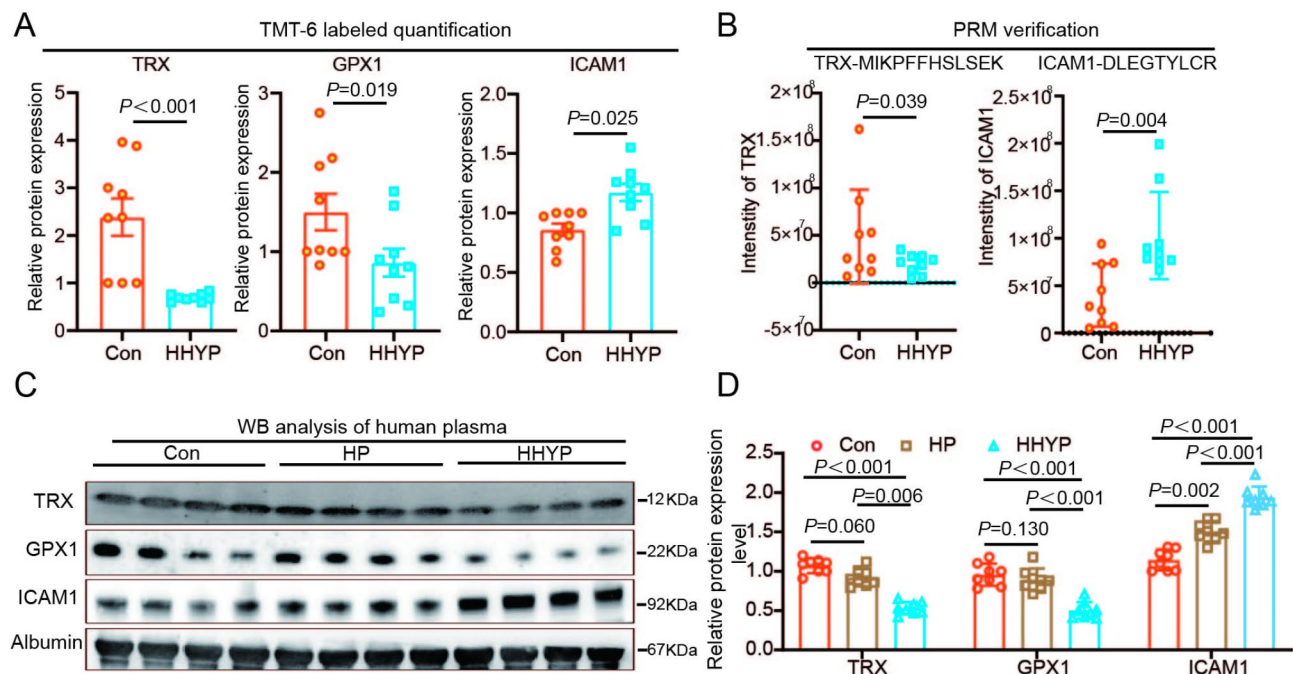*: HP vs. Con; #: HHYP vs. Con; &: HHYP vs. HP

Fig. 3 Validation of differential regulated expression of TRX, GPX1 and ICAM1 in the plasma of HHYP children by using PRM and WB analysis. (**A**) The relative intensity of TRX, GPX1, ICAM1 by TMT6 quantitative method in three replicates. (**B**) The peptide intensities of TRX and ICAM1 as measured by PRM analysis. (**C-D**) WB analysis to validate the expression levels of TRX, GPX1, and ICAM1 in plasma samples from the CON, HP, and HHYP groups. Equal amounts of loading were confirmed by albumin staining. $n = 8$/group

(Fig. 2C, Supplementary Table 2). Considering that vascular endothelial cells can regulate vascular remodeling by sensing blood flow-induced shear stress [18], we postulate that this pathway may be implicated in the etiology of HHYP. Subsequently, we utilized the STRING database to analyze protein-protein interactions (PPI) among the 12 differentially expressed proteins within FSSA pathway. Setting a connectivity degree ≥ 1 and a confidence threshold at 0.9, we established a PPI network using Cytoscape_v3.7.1 (Fig. 2D). Figure 2E illustrates the potential molecular mechanism by which fluid shear stress regulates the function of vascular endothelial cells. Disrupted flow suppresses the TRX and GPX antioxidant system, subsequently triggering the activation of the JNK-NFκB signaling pathway (where inhibited TRX promotes this signaling pathway's activation through apoptosis signal-regulated kinase 1 (ASK1)), leading to an increase in the expression of pro-inflammatory factors like ICAM1 or factors associated with apoptosis. Notably, there is a direct interaction between the TRX and GPX systems, where GPX's antioxidant activity depends on TRX [19–25]. Therefore, we have also categorized GPX1, which was downregulated expression in HHYP, as part of the FSSA pathway. In conclusion, bioinformatics analyses have revealed significant dysregulation in the FSSA pathway in pediatric HHYP.

Verification of differentially expressed proteins in the FSSA pathway of pediatric HHYP patients

Next, we aim to further ascertain whether there is indeed an expression disorder of FSSA pathway proteins in the plasma of pediatric HHYP. Firstly, we employed PRM quantification method in conjunction with Skyline software to analyze the peptide profiles of target proteins in these 9 matched pairs of HHYP patients, with results presented in Supplementary Table 4. The PRM results for TRX, ICAM1, HSP90AA1 were consistent with the findings from TMT6 analysis; however, no difference was observed for RAC1, which is inconsistent with the TMT6 results, however, GPX1 was not detected in the PRM experiment (Fig. 3A-B; Supplementary Fig. 1C). Furthermore, we collected and screened age- and gender-matched plasma samples from 8 cases each of the Con, HP (hypertension without hyperhomocysteinemia), and HHYP groups (Table 2). We used WB technology to verify the differences in the expression of TRX, GPX1, and ICAM1 proteins. The verification results indicated that in the HP group, the expression levels of TRX and GPX1 proteins were not significantly different from those in the Con group, whereas ICAM1 was significantly upregulated. However, in the HHYP group, the expression levels of all three proteins were significantly different compared to both the Con and HP groups (Fig. 3C-D). This suggests that the elevated Hcy may exacerbate these protein expression alterations. Overall, these findings confirm
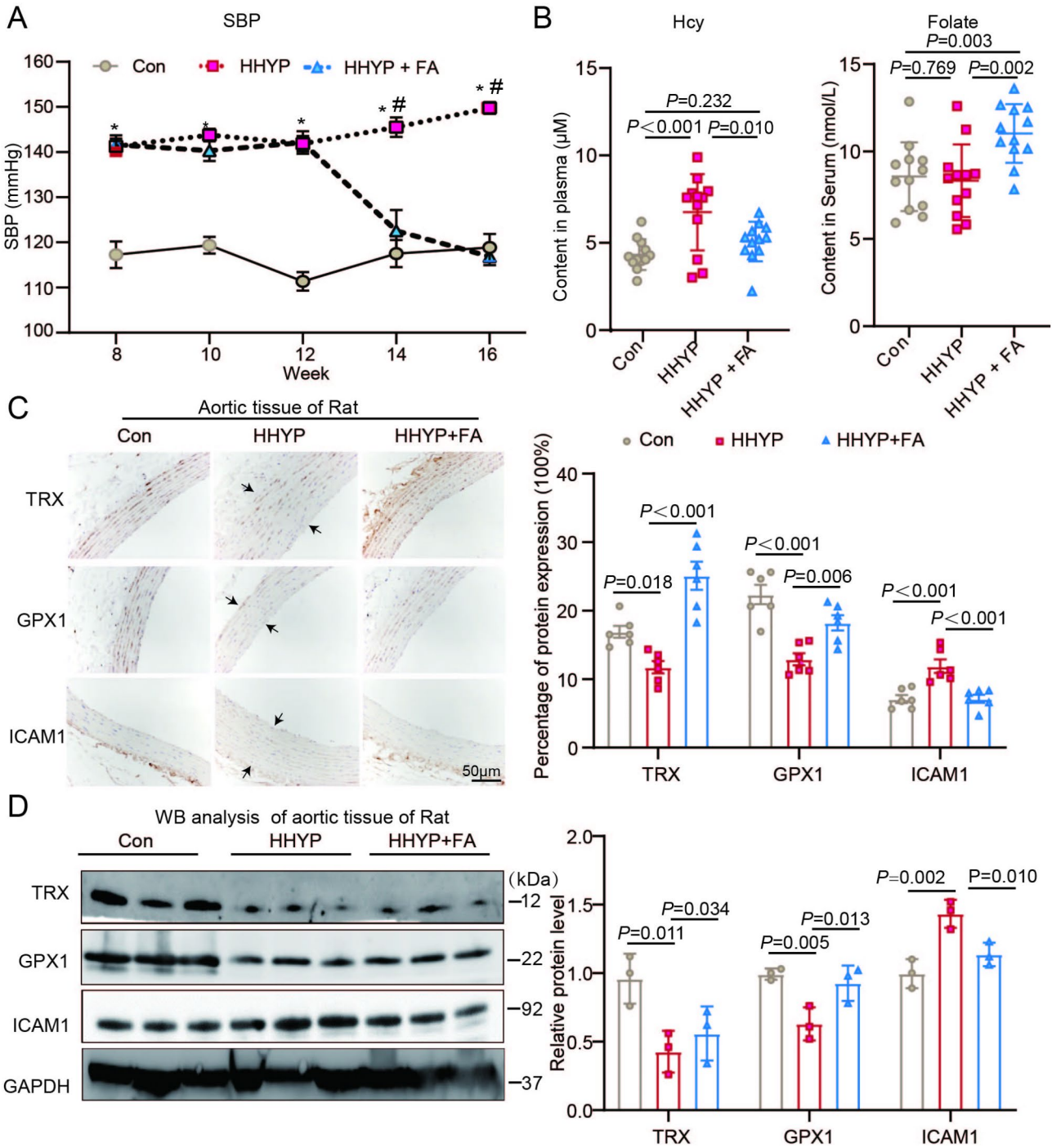
Fig. 4 Decreased TRX, GPX1 and increased ICAM1 expression levels in aorta tissue of HHYP rat model. (**A**) Change of systolic blood pressure (SBP) from 8 to 16 weeks of intervention. (**B**) Hcy content in rat plasma, and folate content in serum (*n* = 12). (**C**) Typical diagram of TRX, GPX1 and ICAM1 protein expression and distribution in rat aorta tissues detected by IHC. Arrows indicate thickened aortic vessels in the HHYP group; Blue indicates the nucleus stained with hematoxylin; brown indicates the staining of target protein (Magnification: X200), *n* = 3, the IHC calculation results for each rat were derived from two fields of view. Bars: 50 µm. (**D**) Representative WB staining bands are shown (TRX, GPX1 and ICAM1). Equal amounts of loading were confirmed by Gapdh staining, *n* = 3/group

the dysregulation of core protein expression in the FSSA pathway within pediatric HHYP.

Dysregulation of the FSSA pathway in an HHYP rat model

To delve deeper into the dysregulation mechanism of the FSSA signaling pathway in HHYP, we established an HHYP rat model by feeding rats with a high methionine
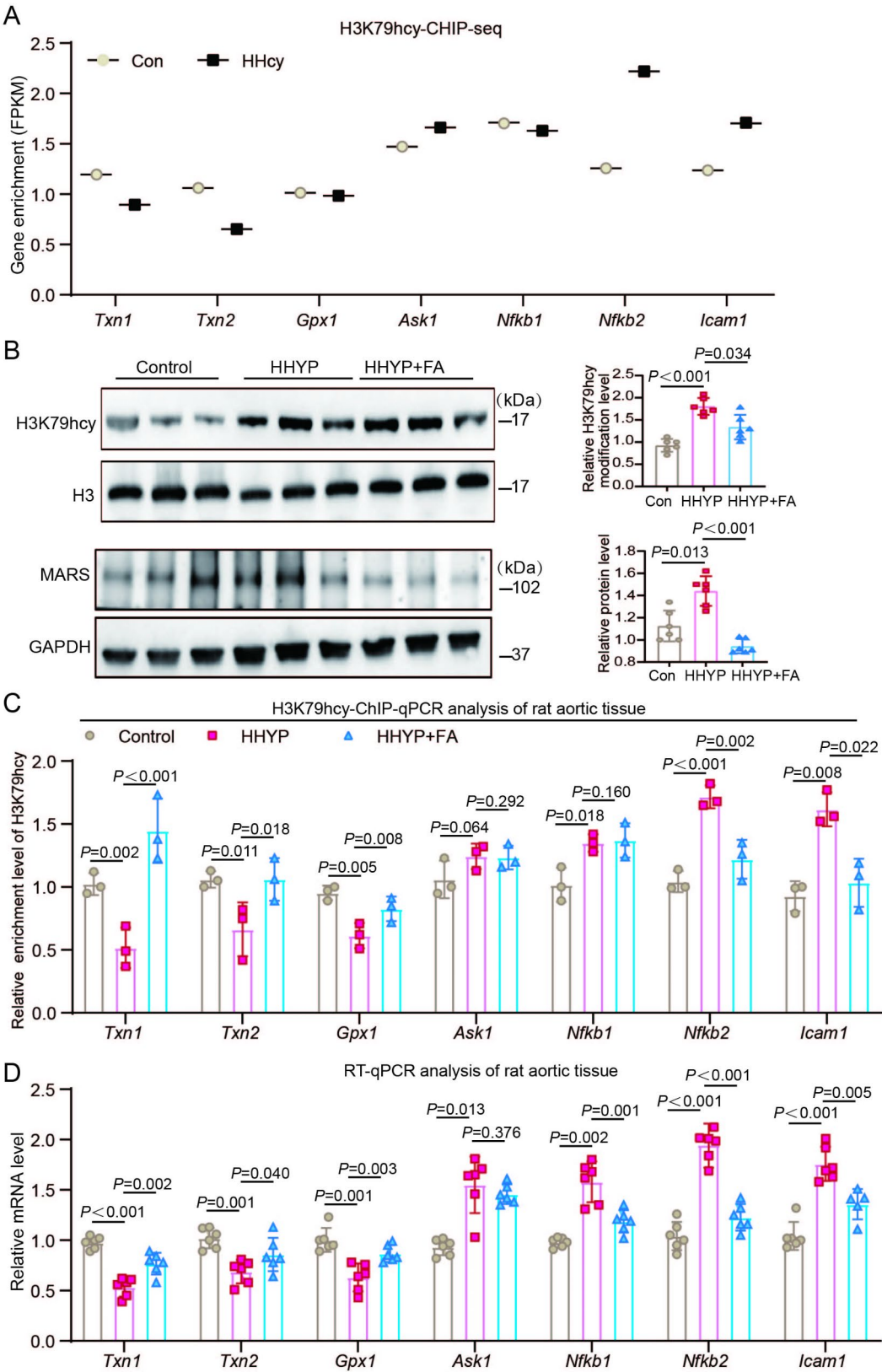
Fig. 5 (See legend on next page.)

(See figure on previous page.)

Fig. 5 Elevated modification of H3K79hcy regulate FSSA pathway genes in aorta tissue of HHYP rats. (**A**) In HHcy treated mouse neural stem cells, H3K79hcy exerts an epigenetic regulatory effect on the genes *Txn1/2*, *Gpx1*, *Ask1*, *Nfkb1/2*, and *Icam1*. (**B**) WB analysis the modification level of H3K79hcy and expression level of MARS protein in rat aortic tissue, $n = 6$. (**C**) The enrichment levels of H3K79hcy in the promoters of TRX pathway genes *Txn1/2*, *Gpx1*, *Ask1*, *Nfkb1/2*, and *Icam1*, which were detected by ChIP-qPCR, $n = 3$. (**D**) RT-qPCR analysis of relative mRNA levels of TRX pathway genes in aorta tissues of the three rat groups (normalized to *Gapdh*), $n = 3$/group, two technical replicates were performed for each sample

diet, as previously reported [26, 27], and additionally set up an experimental group supplemented with FA, a medication currently commonly used in the clinical treatment of HHYP [28], termed HHYP + FA (Supplementary Table 5). Compared to the control group, the SBP of rats in the HHYP group significantly increased from week 8 to week 16, with the most pronounced increase at week 12 (Fig. 4A). Concurrently, HE staining analysis revealed that rats in the HHYP group exhibited arterial wall thickening and disordered myocardial cell arrangement, which were substantially reduced in the HHYP + FA group (Supplementary Fig. 2A). Additionally, we measured the levels of vitamins related to Hcy metabolism in plasma/serum of the different groups. We found that the plasma Hcy content in the HHYP group was 6.75 ± 0.63 μM, significantly higher than in the control group (4.32 ± 0.25 μM) ($P<0.001$). However, the Hcy content (5.07 ± 033 μM) in the HHYP + FA group was substantially lower than that in the HHYP group ($P = 0.010$) (Fig. 4B). There were no significant differences in vitamin B6 and B12 levels between the groups; and folate levels in the HHYP + FA group were higher than those in both the control and HHYP groups (Fig. 4B; Supplementary Fig. 2B-C). These indicators suggest that the HHYP rat model induced by high methionine feeding may primarily be caused by elevated hcy rather than deficiencies in B6/12, and that FA supplementation can effectively mitigate the adverse effects of high Hcy on blood pressure.

Further studies are aimed at confirming whether the dysregulation of the FSSA signaling pathway in the bloodstream originates from changes within the arterial tissue. Initially, using IHC, we examined the expression of relevant proteins in rat aortic and heart tissues. The results showed that the expression of TRX and GPX1 was markedly reduced in the HHYP group but improved in the HHYP + FA group; ICAM1 expression significantly increased in the aortic tissue of the HHYP group but was mitigated after FA supplementation, with no significant changes observed in heart tissue (Figs. 4C; Supplementary Fig. 2D). WB assays further confirmed similar trends in the expression patterns of TRX, GPX1, and ICAM1 across the groups in the aortic tissue (Fig. 4D). These findings indicate that elevated Hcy may serve as the primary trigger for the aberrant expression of TRX/GPX2 and ICAM1, while FA supplementation can offer significant protective effects.

Elevated histone 3 lysine K79 homocysteinylation (H3K79hcy) causes inhibition of TRX and GPX1

Furthermore, we aimed to investigate the mechanisms by which HHcy causes dysregulation of the FSSA pathway. Based on our research group's previous study [29] on the impact of HHcy on gene epigenetic regulation through the upregulation of H3K79hcy, we performed a retrospective analysis of ChIP-seq sequencing data from mouse neural stem cells treated with high Hcy levels. As depicted in Fig. 5A, there was a downward trend in the binding of H3K79hcy to genes such as *Txn1*, *Txn2*, *Gpx1*, and *Nfkb1* under HHcy conditions. In contrast, an upward trend was observed in the binding affinity for *Ask1*, *Nfkb2*, and *Icam1*, suggesting that the increase in H3K79hcy modifications induced by HHcy might be involved in the epigenetic regulation of the FSSA signaling pathways. Following this, we conducted WB analyses using H3K79hcy antibodies on rat aortic tissues. The results showed a significant elevation in H3K79Hcy modification levels in HHYP rats, which significantly decreased following FA treatment in comparison to HHYP rats (Fig. 5B), highlighting abnormalities in H3K79hcy modification in the state of HHYP. Subsequently, using ChIP-qPCR technology, we examined the binding capacity of H3K79hcy to genes like *Txn*. We discovered that the enrichment of H3K79Hcy at the *Txn1*, *Txn2*, and *Gpx1* gene loci was reduced in HHYP rats compared to control rats (Fig. 5C), and this reduction was significantly rescued by FA treatment. Moreover, the binding capacity of H3K79hcy to *Nfkb1*, *Nfkb2*, and *Icam1* was considerably increased in the HHYP group, while the binding levels for *Nfkb2* and *Icam1* were notably diminished after FA supplementation; however, no significant difference was found in the binding of *Ask1* to H3K79Hcy among the groups. Further, we measured mRNA expression levels of these genes and noted a significant decrease in *Txn1*, *Txn2*, and *Gpx1* in the HHYP group, consistent with the protein expression trends shown in Fig. 4; whereas the expression levels of *Nfkb1*, *Nfkb2*, *Ask1*, and *Icam1* were upregulated to varying degrees. FA rescue also had a remedial effect on the expression levels of these genes, except for *Ask1* (Fig. 5D). These findings collectively indicate that H3K79Hcy plays a critical role in regulating gene expression of the FSSA signaling pathway in HHYP rats.
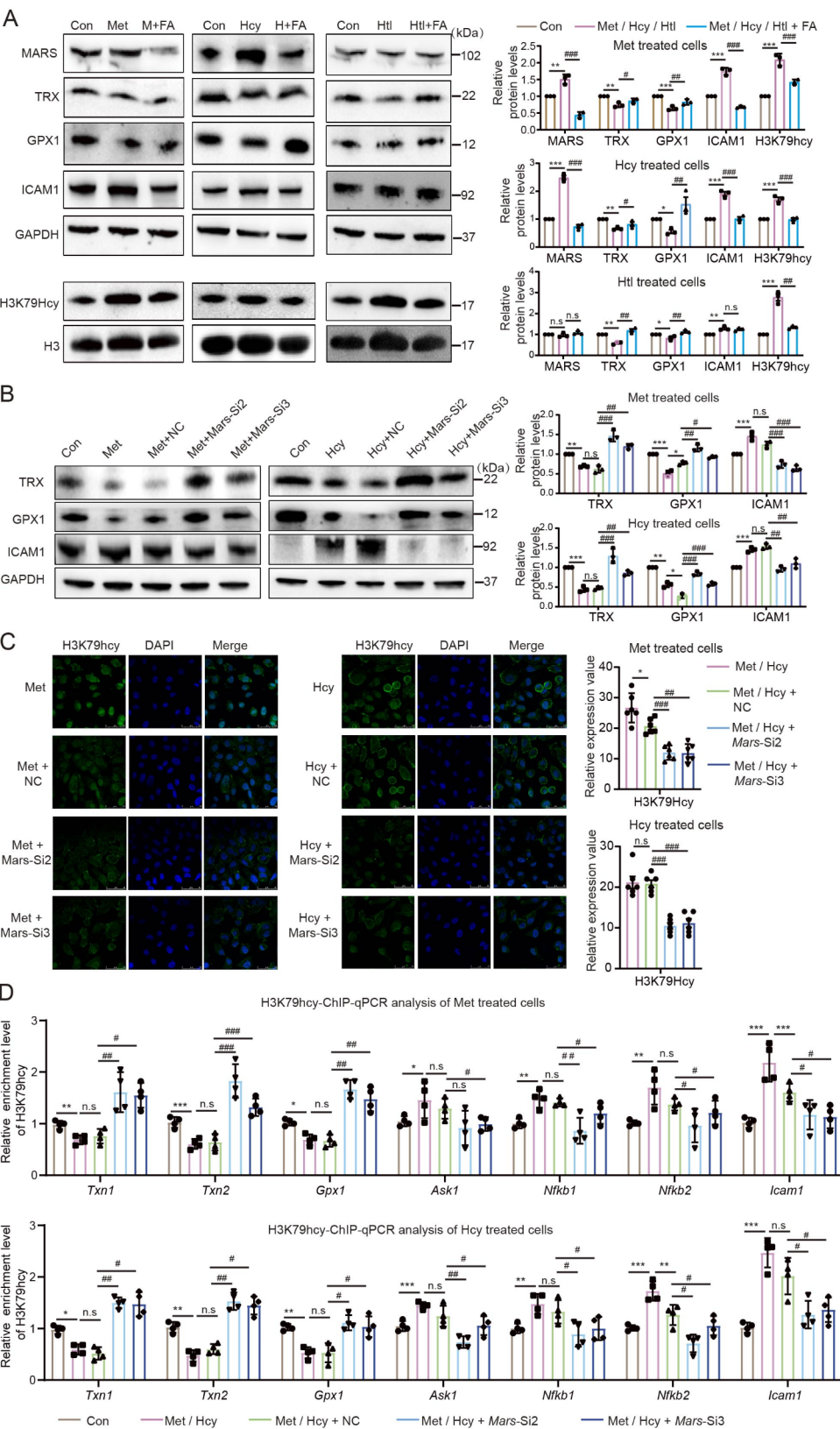
Fig. 6 (See legend on next page.)

(See figure on previous page.)

Fig. 6 *In vitro* experiments confirm that under high methionine or high Hcy environments, histone H3K79hcy abnormal modification occurs and regulates the disordered expression of FSSA genes: (**A**) EAHY926 cells were cultured in vitro with high methionine, high HCY, or high HTL treatments. Western Blot (WB) was used to detect the protein expression levels of MARS, TRX, GPX1, ICAM1, and the modification levels of H3K79hcy. (**B**) In cells treated with high methionine or high HCY, after knocking down MARS expression, protein expression levels of TRX, GPX1, and ICAM1 were detected by Western Blot. (**C**) Immunofluorescence technique was used to detect the expression levels and distribution of H3K79hcy in cells treated with high methionine or high HCY, or in cells where MARS expression was additionally knocked down. (**D**) ChIP-qPCR technique was used to detect the binding ability of H3K79hcy to FSSA pathway genes in cells of different treatment groups

HHcy induces abnormal modification of histone H3K79hcy and regulates FSSA gene expression disorder *in vitro*

To elucidate the impact of HHcy, on H3K79hcy modification and the expression of core proteins such as TRX within the FSSA pathway, we treated cultured human umbilical vein endothelial cells (EAHY926) with high levels of methionine, Hcy, and the metabolic product of Hcy, HTL, respectively. The results revealed that under the influence of these three different reagents, the expression levels of TRX and GPX1 proteins decreased, while ICAM1 expression significantly increased; concurrently, the level of H3K79hcy modification also substantially rose. Experiments in these cell models once again confirmed that high Hcy causes the expression disorder of key proteins in the FSSA pathway.

As MARS protein is an important enzyme for the conversion of Hcy to HTL, its downregulation can inhibit H3K79hcy modification. Therefore, we interfered with MARS expression to further clarify whether Hcy regulates FSSA pathway activity through H3K79hcy modification. Firstly, we found an elevation in MARS expression in the environments of high methionine or Hcy, although there was no change in MARS expression in the HTL treatment group; the addition of FA significantly reversed these changes (Fig. 6A). Hence, it appears that high methionine or Hcy may elevate MARS expression levels, potentially leading to an increase in HTL content and subsequently causing a rise in H3K79hcy modification. To confirm this hypothesis, we selected two siRNAs: si-2 and si-3 against *Mars* gene that showed significant knockdown efficiency (Supplementary Fig. 3A) and conducted a simultaneous knockdown of the *Mars* gene in the presence of methionine or Hcy (Supplementary Figs. 3B-D). The results indicated that in groups where methionine or Hcy treatment was combined with MARS knockdown, compared to groups treated with methionine or Hcy alone, the expression levels of TRX, GPX1, and ICAM1 proteins, as well as the level of H3K79hcy modification, were significantly reversed (Fig. 6B-C). These findings demonstrate the crucial role of MARS in the regulation of H3K79hcy modification and the associated core proteins in the FSSA pathway induced by methionine or Hcy. Finally, using ChIP-qPCR technology, in conditions of high methionine or Hcy and with MARS knocked down, we assessed the binding levels of H3K79hcy to key genes in the FSSA pathway. As shown in Fig. 6D, the knockdown of MARS could reverse the aberrant regulation of genes such as *Txn1/2*, *Gpx1*, *Ask1*, etc., by H3K79hcy caused by high methionine or Hcy. Overall, these data suggest that high levels of Hcy can regulate the modification level of H3K79hcy, then epigenetically controlling the expression of core genes in the FSSA pathway.

Discussion

In this study, we presented a quantitative proteomic landscape of children with HHYP. Through bioinformatics analysis, we focused on the FSSA pathway and observed downregulation of TRX and GPX proteins, along with upregulation of ICAM1 protein in child HHYP cases. Furthermore, using a rat HHYP model, we validated dysregulation of the FSSA pathway in rat aortic tissues, likely due to epigenetic regulation from elevated H3K79hcy levels induced by HHcy. Finally, we confirmed in an in vitro cultured cell model that high Hcy epigenetically regulates the activity of the FSSA pathway by upregulating H3K79hcy modification. These results suggest a possible pathogenic mechanism underlying the occurrence of HHYP.

At present, deficiencies in folate, vitamin B12/B6, or key enzyme gene mutations/function loss in Hcy metabolism have been reported to cause HHcy; however, their precise relationship with each other and hypertension remains unclear. In children's HHYP plasma samples, we observed significantly lower levels of folate and B12, alongside remarkable HHcy, suggesting that deficiencies in folate and B12 could be contributing factors to clinical HHcy [9, 10]. Furthermore, we developed an HHYP rat model fed with methionine. Results from Fig. 4A-B indicate that HHcy may play a crucial role in the pathological process of hypertension induced by methionine intake as well as in the therapeutic approach involving folate for hypertension. It has been challenging to determine the independent impact of HHcy on hypertension since HHcy typically coexists with various dietary and lifestyle risk factors [30, 31]. Nevertheless, an epidemiological study demonstrated a strong association between HHcy and hypertension: with every 5μM increase in plasma hcy, there was an increase of 0.7/0.5 mmHg in SBP or DBP for men and 1.2/0.7 mmHg for women, which was independent of B vitamin status [30], indicating a weak correlation between serum vitamin B12/6 and hypertension [32]. These results suggest a pivotal role of HHcy in inducing hypertension, lowering the level of Hcy might

be one of the mechanisms of FA supplementation to protect against hypertension.

Dysregulation of TRX expression has been reported in various hypertensive rat models, such findings have rarely been confirmed in humans [33–35]. Our study found that TRX protein expression is also suppressed in plasma samples from children with HHYP and in aortic tissue of HHcy-induced hypertensive rats (Figs. 3 and 4). TRX primarily plays a role in regulating cellular inflammation;; reduced TRX levels under conditions of disturbed blood flow may lead to the activation of ASK1 and IκB degradation, culminating in the activation of NFκB and AP-1 transcription factors. These factors are instrumental in elevating the expression of the pro-inflammatory gene ICAM1 [36]. ICAM1 has been reported to play a critical role in mediating leukocyte adhesion and infiltration in the vascular endothelium. Elevated levels of ICAM1 can enhance the attachment of leukocytes to endothelial cells, promoting their transmigration into the intima. This process results in chronic inflammation, which is a key factor in the development of atherosclerotic plaques. Therefore, the increased expression of ICAM1 likely facilitates the inflammatory response and exacerbates plaque formation [37, 38]. This TRX-ICAM1 pathway might explain the involvement of the FSSA pathway in the pathogenesis of HHYP. as depicted in Fig. 7.

In addition, TRX also act as a major cellular redox protein, is responsible for neutralizing reactive oxygen species (ROS) within vascular cells [19, 39], administration of recombinant human TRX (rhTRX) to aged wild-type mice could alleviate hypertension, with effects lasting several days [19, 39]. These findings suggest that TRX downregulation may contribute to hypertension induction, while elevating TRX levels can offer protective benefits against hypertension.GPX1, another important antioxidant enzyme, was found to have significantly reduced expression in a rat model of hypertension induced by selenium-deficient feeding. It is involved in the regulation of renal AT1R expression through modulating the expression and activity of NF-κB p65, which may be one mechanism by which GPX1 participates in the development of hypertension [40]. Furthermore, reports suggest that there may be an interaction between TRX and GPX1. TRX serves as an electron donor for the GPX1 enzyme, when subjected to fluid shear stress, GPX1 reduces the activation of the JNK-NFκB signaling pathway, helping to mitigate oxidative stress [21, 25, 41]. Specifically, elevated Hcy levels lead to reduced expression of TRX and GPX1, which in turn results in the excessive accumulation of ROS, causing oxidative damage to endothelial cells. This oxidative stress disrupts endothelial function, impairs nitric oxide (NO) production, and promotes endothelial dysfunction. The resulting environment further favors the initiation and progression of atherosclerosis by enhancing lipid peroxidation, vascular smooth muscle cell proliferation, and further inflammatory cell recruitment [42–44]. Moreover, in the aortic tissues of rats with HHcy-induced atherosclerosis, researchers also observed
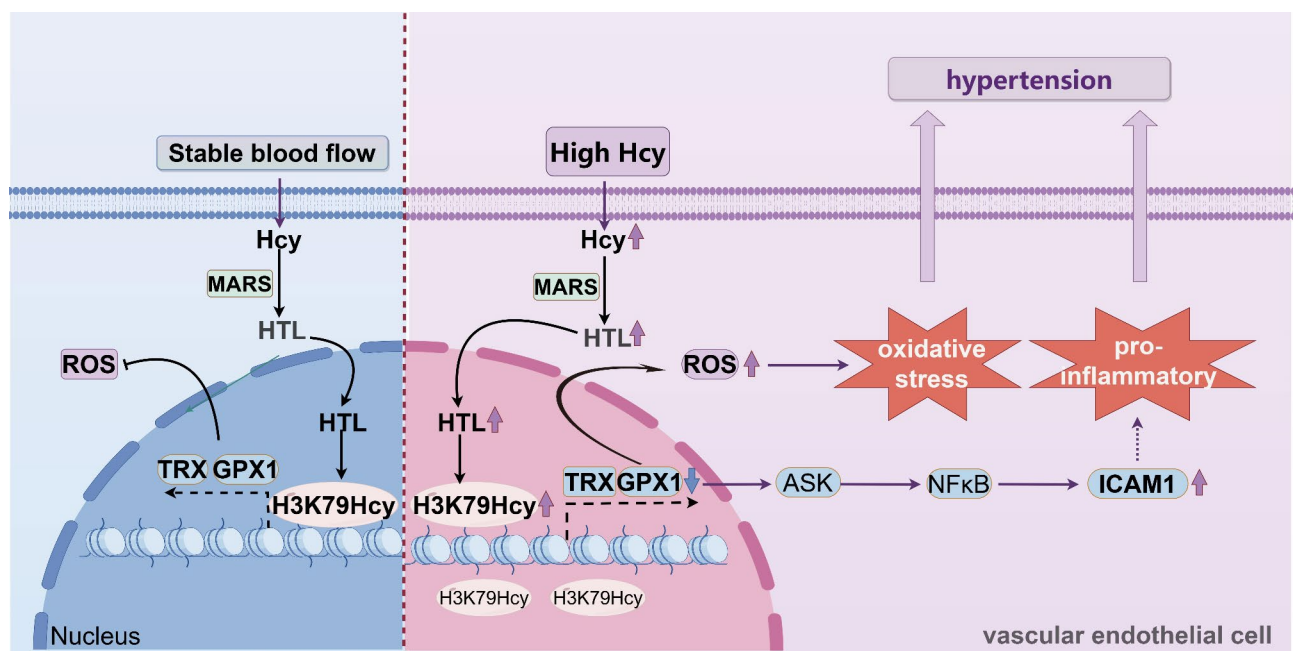

Fig. 7 The schematic diagram illustrates the mechanism by which high Hcy levels promote hypertension. This occurs through the upregulation of H3K79hcy modifications, thereby epigenetically regulating the expression of TRX, GPX1, and related pathway factors such as NFkB to enhance oxidative stress, or by stimulating inflammation via the upregulation of ICAM1

a simultaneous reduction in GPX1 expression and an increase in ICAM1 expression. raising the question of whether there is mutual regulation between them; Based on the information above, we hypothesize that the inhibition of TRX may synergize with GPX1 to increase oxidative stress, or potentially upregulate ICAM1 to promote an inflammatory response, thereby jointly contributing to the onset of HHYP.

A remaining question is how HHcy inhibits TRX/GPX1 while activating ICAM1 in HHYP. After exposing isolated adult rat ventricular myocytes to Hcy for 24 h, the levels of TRX protein decrease [45]; At the same time, HHcy inhibits the expression of the GPX1 both in vitro and in vivo [46], suggesting a correlation between HHcy, TRX and GPX1 inhibition. The elevation of H3K79hcy caused by HHcy is found to be associated with the binding of *Txn1/2* genes encoding TRX proteins [29]. In our study, we identified an increase in H3K79hcy in the aortic tissue of HHYP rats, accompanied by a reduction in the binding levels of H3K79hcy to *Txn1*, *Txn2*, and *Gpx1* genes, conversely, there was a marked increase in the enrichment of H3K79hcy with downstream genes including *Ask1*, *Nfkb1*, *Nfkb2*, and *Icam1*. This suggests that H3K79hcy may exert distinct patterns of epigenetic regulation on these genes (Fig. 5). Furthermore, in the cell model, we confirmed that MARS protein is the central protein mediating the epigenetic regulation of FSSA genes by H3K79hcy induced by high methionine or high Hcy (Fig. 6). However, whether FSSA pathway related proteins also undergo homocysteinylation as a post-translational modification, which in turn affects their abnormal protein expression [14, 15], warrants further investigation.

Finally, to further explore the pathogenic mechanisms of hypertension related to high hcy levels, we have also constructed an interaction network map of 182 differentially expressed proteins involved in 69 altered pathways (Supplementary Fig. 1D). Our investigation specifically focuses on two pathways related to Hcy metabolism: Cysteine and methionine metabolism and Glutathione metabolism; and those associated with hypertension pathogenesis: Complement and Coagulation Cascades, Fluid Shear Stress and Atherosclerosis, Lipid and atherosclerosis, Pathways of Neurodegeneration - Multiple Diseases, Platelet Activation, Dilated cardiomyopathy, Focal adhesion and Ras Signaling Pathway. We observed that some key differentially expressed proteins, such as HSP90AA1, ENO1, and CDC42, play significant roles in the interactions among different pathways. Additionally, some proteins with significant differential expression in HHYP (ranked among the top 20), such as SERPIND1, C6, C9, and RAP1B, also participate in these important pathways and their interactions. This suggests that these proteins may together play key roles in the complex pathogenic mechanisms of hypertension related to high Hcy levels. These findings warrant further exploration and investigation in future studies.

In summary, quantitative proteomics analysis may provide a more functionally-oriented approach for identifying novel models or pathways potentially involved in the development of pediatric HHYP. Our data suggest that alterations in FSSA pathway proteins are significant contributors to the pathogenesis of HHYP. However, how these proteins interact with each other to induce the occurrence of HHYP still requires further exploration, so as to improve the understanding of the treatment mechanism of HHYP and provide targets for the prevention and treatment of HHYP.

Supplementary Information

The online version contains supplementary material available at https://doi.org/10.1186/s12967-025-06483-6.

Supplementary Material 1: **Supplementary Fig. 1**. (A) GO analysis reveals the altered proteins more preferable enrich in cellular process and play roles in binding and catalytic activity. (B) KEGG analysis of the top 20 signaling pathways enriched by upregulated expressed proteins. (C) The relative intensity of HSP90AA1, RAC1 by TMT6 quantitative method in three replicates (Upper part) and the peptide intensities as measured by PRM analysis (Lower part). (D)In the figure, the interactions between differential proteins in 69 significantly enriched pathways are displayed. The size of the spheres indicates the strength of interaction of the protein within the entire network; the larger the sphere, the higher its interaction strength. **Supplementary Fig. 2**. (A) The classic signaling pathway diagram of the Fluid Shear Stress Pathway (from KEGG). (B)HE staining of rat aorta and heart tissues. (C-D) Vitamine B12/6 content in rat serum, *n*=12/group. (E) IHC analysis of TRC, GPX1, ICAM1 protein expression pattern in heart tissues of rat model, *n*=3. **Supplementary Fig. 3**. Knocking down MARS expression in EAHY926 cells. (A) In normally cultured EAHY926 cells, transfection with empty vector (NC), mars knockdown plasmids si-1, si-2, si-3, and si1+2+3, the efficiency of MARS protein knockdown was detected by WB. (B-D) Immunofluorescence technique was used to detect the expression levels and distribution of MARS protein in cells treated with high methionine or high Hcy after transfection with NC or *Mars* gene knockdown plasmids si-2 and si-3.

Supplementary Material 2

Declarations

Ethics approval and consent to participate
All human subjects received informed consent and the study was approved by the medical ethics committee of the Capital Institute of Pediatrics (Beijing, China) (SHERLL2022017), conducted in accordance with the Helsinki Declaration of 1975 (as revised in 2008) concerning Human and Animal Rights, and that they followed out the policy concerning Informed Consent as shown on Springer.com. Animal research was approved by the animal ethics committee of Capital Institute of Pediatrics (DWLL2021004).

Consent for publication
Not applicable.

Competing interests
The authors declare that they have no competing interests.

Author details
[1]Beijing Municipal Key Laboratory of Child Development and Nutriomics, Capital Institute of Pediatrics, No. 2 Yabao Rd, Beijing 100020, China
[2]Department of Cardiology, Capital Center for Children's Health, Capital Medical University, No. 2 Yabao Rd, Beijing 100020, China

References
1. Falkner B. The enigma of primary hypertension in childhood. Front Cardiovasc Med. 2022;9:1033628.
2. Lee CG. The emerging epidemic of hypertension in Asian children and adolescents. Curr Hypertens Rep. 2014;16(12):495.
3. Chen C, Lu M, Wu Y, Zhang Z, Hu J, Yin J, et al. The prevalence of hypertension and elevated blood pressure and its correlation with overweight/obesity among students aged 6–17 years in Suzhou. Journal of pediatric endocrinology & metabolism: JPEM; 2021.
4. Song P, Zhang Y, Yu J, Zha M, Zhu Y, Rahimi K, et al. Global prevalence of hypertension in children: A systematic review and Meta-analysis. JAMA Pediatr. 2019;173(12):1154–63.
5. de Almeida A, Ribeiro TP, de Medeiros IA. Aging: molecular pathways and implications on the cardiovascular system. Oxid Med Cell Longev. 2017;2017:7941563.
6. Hu F, Yu S, Li J, Zhou W, Wang T, Huang X, et al. Association between hyperhomocysteinemia combined with metabolic syndrome and higher prevalence of stroke in Chinese adults who have elevated blood pressure. Med Sci Monitor: Int Med J Experimental Clin Res. 2022;28:e934100.
7. Rodrigo R, Passalacqua W, Araya J, Orellana M, Rivera G. Homocysteine and essential hypertension. J Clin Pharmacol. 2003;43(12):1299–306.
8. Tu W, Yan F, Chao B, Ji X, Wang L. Status of hyperhomocysteinemia in China: results from the China stroke High-risk population screening program, 2018. Front Med. 2021;15(6):903–12.
9. Kaye AD, Jeha GM, Pham AD, Fuller MC, Lerner ZI, Sibley GT, et al. Folic acid supplementation in patients with elevated homocysteine levels. Adv Ther. 2020;37(10):4149–64.
10. Zhang L, Li Z, Xing C, Gao N, Xu R. Folate reverses NF-κB p65/Rela/IL-6 level induced by hyperhomocysteinemia in spontaneously hypertensive rats. Front Pharmacol. 2021;12:651582.
11. Stanger O, Herrmann W, Pietrzik K, Fowler B, Geisel J, Dierkes J, et al. Clinical use and rational management of homocysteine, folic acid, and B vitamins in cardiovascular and thrombotic diseases. Z Kardiol. 2004;93(6):439–53.
12. Zhang S, Wang T, Wang H, Tang J, Hou A, Yan X, et al. Effects of individualized administration of folic acid on prothrombotic state and vascular endothelial function with H-type hypertension: A double-blinded, randomized clinical cohort study. Medicine. 2022;101(3):e28628.
13. Zhao F, Li JP, Wang SY, Guan DM, Ge JB, Hu J, et al. [The effect of baseline homocysteine level on the efficacy of Enalapril maleate and folic acid tablet in Lowering blood pressure and plasma homocysteine]. Zhonghua Yi Xue Za Zhi. 2008;88(42):2957–61.
14. Balint B, Jepchumba VK, Guéant JL, Guéant-Rodriguez RM. Mechanisms of homocysteine-induced damage to the endothelial, medial and adventitial layers of the arterial wall. Biochimie. 2020;173:100–6.
15. Gurda D, Handschuh L, Kotkowiak W, Jakubowski H. Homocysteine Thiolactone and N-homocysteinylated protein induce pro-atherogenic changes in gene expression in human vascular endothelial cells. Amino Acids. 2015;47(7):1319–39.
16. Zhang K, Liu Y, Liu L, Bai B, Shi L, Zhang Q. Untargeted metabolomics analysis using UHPLC-Q-TOF/MS reveals metabolic changes associated with hypertension in children. Nutrients. 2023;15(4).
17. Zhang Q, Wu L, Bai B, Li D, Xiao P, Li Q, et al. Quantitative proteomics reveals association of neuron projection development genes ARF4, KIF5B, and RAB8A with hirschsprung disease. Mol Cell Proteom. 2021;20:100007.
18. Baeyens N, Bandyopadhyay C, Coon BG, Yun S, Schwartz MA. Endothelial fluid shear stress sensing in vascular health and disease. J Clin Investig. 2016;126(3):821–8.
19. Hilgers RH, Kundumani-Sridharan V, Subramani J, Chen LC, Cuello LG, Rusch NJ et al. Thioredoxin reverses age-related hypertension by chronically improving vascular redox and restoring eNOS function. Sci Transl Med. 2017;9(376).
20. Liu Q, Yang J, Cai J, Luan Y, Sattar H, Liu M, et al. Analysis of the interactions between thioredoxin and 20 selenoproteins in chicken. Biol Trace Elem Res. 2017;179(2):304–17.
21. Hojo Y, Saito Y, Tanimoto T, Hoefen RJ, Baines CP, Yamamoto K, et al. Fluid shear stress attenuates hydrogen peroxide-induced c-Jun NH2-terminal kinase activation via a glutathione reductase-mediated mechanism. Circul Res. 2002;91(8):712–8.
22. Boamah GA, Huang Z, Shen Y, Lu Y, Wang Z, Su Y, et al. Transcriptome analysis reveals fluid shear stress (FSS) and atherosclerosis pathway as a candidate molecular mechanism of short-term low salinity stress tolerance in abalone. BMC Genomics. 2022;23(1):392.
23. Yamawaki H, Pan S, Lee RT, Berk BC. Fluid shear stress inhibits vascular inflammation by decreasing thioredoxin-interacting protein in endothelial cells. J Clin Investig. 2005;115(3):733–8.
24. Zhou J, Li YS, Chien S. Shear stress-initiated signaling and its regulation of endothelial function. Arterioscler Thromb Vasc Biol. 2014;34(10):2191–8.
25. Ahmad F, Latif MF, Luo Y, Huang Y. Basis for using thioredoxin as an electron donor by Schizosaccharomyces Pombe Gpx1 and Tpx1. AMB Express. 2022;12(1):41.
26. Lu F, Zhao LY, Zhang ZM, Zou Q, Yu XL, Wei CY. The intervention of Enalapril maleate and folic acid tablet on the expressions of the GRP78 and CHOP and vascular remodeling in the vascular smooth muscle cells of H-hypertensive rats with homocysteine. Eur Rev Med Pharmacol Sci. 2018;22(7):2160–8.
27. Zhang DH, Wen XM, Zhang L, Cui W. DNA methylation of human telomerase reverse transcriptase associated with leukocyte telomere length shortening in hyperhomocysteinemia-type hypertension in humans and in a rat model. Circulation Journal: Official J Japanese Circulation Soc. 2014;78(8):1915–23.
28. Bao H, Huang X, Li P, Sheng C, Zhang J, Wang Z, et al. Combined use of amlodipine and folic acid are significantly more efficacious than amlodipine alone in Lowering plasma homocysteine and blood pressure among hypertensive patients with hyperhomocysteinemia and intolerance to ACEI: A multicenter, randomized, double-blind, parallel-controlled clinical trial. J Clin Hypertens (Greenwich Conn). 2023;25(8):689–99.
29. Zhang Q, Bai B, Mei X, Wan C, Cao H, Dan L, et al. Elevated H3K79 homocysteinylation causes abnormal gene expression during neural development and subsequent neural tube defects. Nat Commun. 2018;9(1):3436.
30. Stehouwer CD, van Guldener C. Does homocysteine cause hypertension? Clin Chem Lab Med. 2003;41(11):1408–11.
31. Dinavahi R, Falkner B. Relationship of homocysteine with cardiovascular disease and blood pressure. J Clin Hypertens (Greenwich Conn). 2004;6(9):494–8. quiz 9-500.
32. van Guldener C, Nanayakkara PW, Stehouwer CD. Homocysteine and blood pressure. Curr Hypertens Rep. 2003;5(1):26–31.
33. Whayne TF Jr., Parinandi N, Maulik N. Thioredoxins in cardiovascular disease. Can J Physiol Pharmacol. 2015;93(11):903–11.
34. Das KC, Kundumani-Sridharan V, Subramani J. Role of thioredoxin in Age-Related hypertension. Curr Hypertens Rep. 2018;20(1):6.

35. Ebrahimian T, Touyz RM. Thioredoxin in vascular biology: role in hypertension. Antioxid Redox Signal. 2008;10(6):1127–36.
36. Nigro P, Abe J, Berk BC. Flow shear stress and atherosclerosis: a matter of site specificity. Antioxid Redox Signal. 2011;15(5):1405–14.
37. Ni Y, Cao J, Li Y, Qi X. SOX11 silence inhibits atherosclerosis progression in ApoE-deficient mice by alleviating endothelial dysfunction. Exp Cell Res. 2025;445(1):114422.
38. Xie BL, Bie YL, Song BC, Liu MW, Yang L, Liu J et al. Zedoarondiol inhibits monocyte adhesion and expression of VCAM and ICAM in endothelial cells induced by oxidative stress. Nat Prod Res. 2024;9:1–7.
39. Kundumani-Sridharan V, Subramani J, Das KC. Thioredoxin Activates MKK4-NFκB Pathway in a Redox-dependent Manner to Control Manganese Superoxide Dismutase Gene Expression in Endothelial Cells. J Biol Chem. 2015;290(28):17505–19.
40. Lei L, Zhang F, Huang J, Yang X, Zhou X, Yan H, et al. Selenium deficiency causes hypertension by increasing renal AT(1) receptor expression via GPx1/H(2)O(2)/NF-κB pathway. Free Radic Biol Med. 2023;200:59–72.
41. Wang S, Wang M, Zhang S, Zhao L. Oxidative stress in rats with hyperhomocysteinemia and intervention effect of lutein. Eur Rev Med Pharmacol Sci. 2014;18(3):359–64.
42. Lubos E, Loscalzo J, Handy DE. Glutathione peroxidase-1 in health and disease: from molecular mechanisms to therapeutic opportunities. Antioxid Redox Signal. 2011;15(7):1957–97.
43. He L, Zhang Y, Fang Y, Liang W, Lin J, Cheng M. Classical swine fever virus induces oxidative stress in swine umbilical vein endothelial cells. BMC Vet Res. 2014;10:279.
44. De Miguel C, Pelegrín P, Baroja-Mazo A, Cuevas S. Emerging role of the inflammasome and pyroptosis in hypertension. Int J Mol Sci. 2021;22(3).
45. Abdel-Magied N, Shedid SM. Impact of zinc oxide nanoparticles on thioredoxin-interacting protein and asymmetric dimethylarginine as biochemical indicators of cardiovascular disorders in gamma-irradiated rats. Environ Toxicol. 2020;35(4):430–42.
46. Weiss N, Zhang YY, Heydrick S, Bierl C, Loscalzo J. Overexpression of cellular glutathione peroxidase rescues homocyst(e)ine-induced endothelial dysfunction. Proc Natl Acad Sci USA. 2001;98(22):12503–8.

Publisher's note